[3] G. Nuzillat, "GaAs IC technology for ultra-high speed digital systems," in *URSI XXIst General Assembly Dig.* (Florence, Italy), Aug. 28–Sept. 5, 1984, p. 496.
[4] K. E. Meyer, D. R. Dykarr, and G. A. Mourou, "Characterization of TEGFETS and MESFETS using the electro-optic sampling technique," in *Picosecond Electronics and Optoelectronics Topical Meeting Proc.*, 1985, p. 54.
[5] D. R. Dykarr *et al.*, "Picosecond electro-optic characterization of the permeable base transistor," in *1986 Dig. Conf. Lasers and Electro-Optics* (San Francisco, CA), June 9–13, 1986, p. 314.
[6] R. A. Lawton, "Pulse waveform standards for electro-optics," in *Picosecond Electronics and Optoelectronics Topical Meeting Proc.*, 1985, p. 205.
[7] W. L. Gans, "The measurement and deconvolution of time jitter in equivalent-time waveform samplers," *IEEE Trans. Instrum. Meas.*, vol. IM-32, no. 1, pp. 126–133, Mar. 1983.
[8] N. S. Nahman, *et al*, "Applications of time domain methods to microwave measurements," *Proc. Inst. Elec. Eng.*, vol. 127, pt. H, no. 2, pp. 99–106, Apr. 1980.

New Quasi-Static Models for the Computer-Aided Design of Suspended and Inverted Microstrip Lines

R. S. TOMAR, MEMBER, IEEE, AND
PRAKASH BHARTIA, SENIOR MEMBER, IEEE

Abstract —**New quasi-static models for the computer-aided design (CAD) and analysis of open suspended and inverted microstrip lines are reported. The models are obtained through generalizing those reported earlier and are applicable up to $\epsilon_r = 20$, thereby covering all the practically used substrate materials for these structures. The models also cover a larger range of dimension ratios and are accurate to within 0.6 percent for analysis and within 1 percent for synthesis.**

I. Introduction

Suspended and inverted microstrip lines are among the principal transmission media used in the upper microwave and lower millimeter-wave bands. The cross sections of these lines are shown in Fig. 1, with parameters W, a, b, ϵ_r, and t defined therein. The most interesting aspect of these lines is that the presence of an air gap between the substrate and the ground plane reduces the effects of dispersion on the propagation constant, generally to such an extent that the quasi-static results remain useful even at very high frequencies. For instance, with RT-duroid substrate ($\epsilon_r = 2.22$), a suspended microstrip structure with $W = a = b$ displays only about 7 percent variation in the guided wavelength when the frequency is varied from 1 GHz to 100 GHz. Keeping this feature in mind, much effort has been devoted in the past few years to developing accurate quasi-static models for the computer-aided design and analysis of these lines [1]–[4]. The effects of manufacturing tolerances on the electrical performance have also been studied [5].

The CAD models developed in [1]–[4], and used subsequently in [5], are accurate to within 1 percent of the rigorously obtained theoretical data, provided the parameters stay within the range $1 \leqslant W/b \leqslant 8$, $0.2 \leqslant a/b \leqslant 1$, and $\epsilon_r \leqslant 3.8$. the restriction $\epsilon_r \leqslant 3.8$ is particularly serious because substrates with $\epsilon_r \geqslant 3.8$, e.g., alumina ($\epsilon_r = 9.6$) and GaAs ($\epsilon_r = 12.9$), are often used in practice. The aim of this paper is to report new generalized quasi-static models valid up to $\epsilon_r = 20$. Over the range $0.5 \leqslant W/b \leqslant 10$, $0.05 \leqslant a/b \leqslant 1.5$, the accuracy of these models (in reproducing the exact theoretical data) is generally better than 0.6 percent for analysis and better than 1 percent for synthesis.

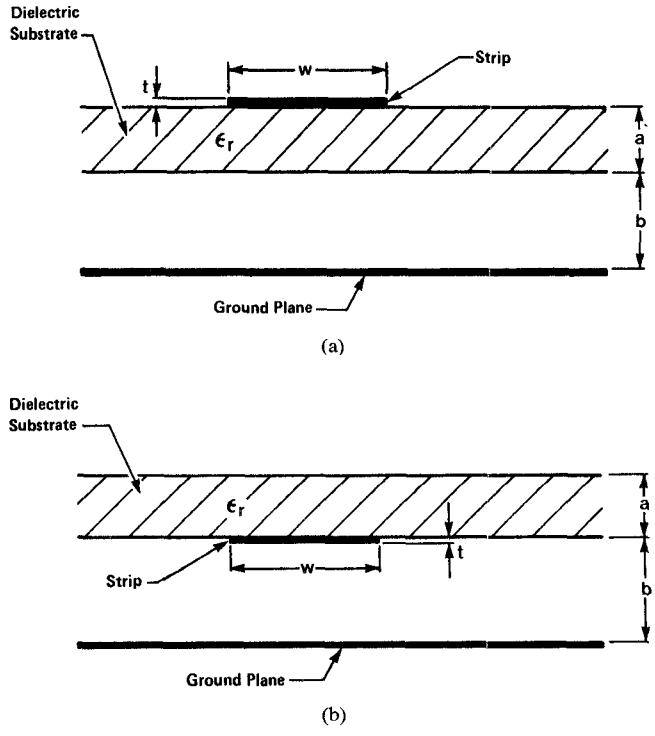

Fig. 1. Cross sections of (a) suspended and (b) inverted microstrip lines.

Like the earlier models [1]–[4], the present models too are developed using the technique of least-square curve fitting to exact theoretical data, which in turn are generated using the variational approach in the Fourier transform domain.[1] (For details of this approach, see, e.g., [6] and [7].) It should also be mentioned that the present work relies on the use of the W/b term (instead of $\ln(W/b)$ term, which was used in [1]–[4]) for modeling the effective dielectric constant. The present models thus do not break down for $W/b \leqslant 1$, as was the case with the earlier models.

II. Models for Analysis

In this section, new models for analyzing the suspended and inverted microstrip structures are presented.

A. Suspended Microstrip

The effective dielectric constant is given by

$$\sqrt{\epsilon_{re}} = (1 - f_1 f_2)^{-1} \tag{1}$$

where

$$f_1 = 1 - \frac{1}{\sqrt{\epsilon_r}} \tag{2}$$

[1]This approach has been shown to yield good agreement with the experimental results [7].

Manuscript received July 23, 1986; revised November 28, 1986. This work was supported in part by the Natural Sciences and Engineering Research Council of Canada under Grant A-0001.

R. S. Tomar was with the Department of Electrical Engineering, University of Ottawa, Ottawa, Canada. He is now with Bolriet Technologies, Inc., Carleton Place, Ontario, Canada K7C 3P3.
P. Bhartia is with the Department of National Defence, On OT Ottawa, Ontario, Canada K1A 0K2.

IEEE Log Number 8612955.

and

$$f_2^{-1} = \sum_{i=0}^{3} c_i (w/b)^i. \tag{3}$$

The functions C_i in (3) are given by

$$C_i = \sum_{j=0}^{3} d_{ij} \left(\frac{b}{a}\right)^j \tag{4}$$

where the d coefficients are known functions of ϵ_r (see the Appendix).

The above model differs from its counterpart in [1]–[4] in that the function f_2 has been assumed to depend not only on W/b and a/b but also on ϵ_r.

Once ϵ_{re} is known, the impedance Z can be computed using the well-known equation

$$Z = Z_0/\sqrt{\epsilon_{re}} \tag{5}$$

where Z_0, the impedance of an identical air-filled line, is given by Hammerstad and Jensen's equation [8], [9]:

$$Z_0 = 60 \ln\left[\frac{f(u)}{u} + \sqrt{1+\frac{4}{u^2}}\right] \tag{6}$$

with

$$u = \frac{W/b}{1+(a/b)} \tag{7}$$

and

$$f(u) = 6 + (2\pi - 6)\exp\left[-(30.666/u)^{0.7528}\right]. \tag{8}$$

B. Inverted Microstrip

In this case, the effective dielectric constant is written as

$$\sqrt{\epsilon_{re}} = 1 + f_1 f_2 \tag{9}$$

where

$$f_1 = \sqrt{\epsilon_r} - 1 \tag{10}$$

and f_2 is given by (3) and (4), with the d's again defined in terms of ϵ_r (see the Appendix).

Like eq. (1), eq. (9) too differs from its counterpart in [1]–[4] in that the function f_2 is assumed to depend on all three of the quantities W/b, a/b, and ϵ_r.

The inverted line impedance can also be computed using (5), (6), and (8), with u defined by

$$u = W/b \tag{11}$$

in place of (7).

III. Models for Synthesis

The synthesis problem consists of finding W/b for a given ϵ_r, a/b, and Z. As was discussed in [3] and [4], a very simple synthesis technique, accurate to within 0.4 percent of the analytical results, emerges if (8) is replaced by the approximation

$$f(u) = 6 \tag{12}$$

since (12) simplifies the inversion of (5) to a considerable extent. In the present instance, the use of this procedure leads to the following synthesis equations.

A. Suspended Microstrip

Defining

$$x = \frac{1}{u} = \frac{1+(a/b)}{W/b} \tag{13}$$

we get

$$f(x)\ln\left(6x + \sqrt{1+4x^2}\right) = Z/60 \tag{14}$$

where

$$f(x) = 1 - \frac{x^3\left(1 - \frac{1}{\sqrt{\epsilon_r}}\right)}{C_0' x^3 + C_1' x^2 + C_2' x + C_3'} \tag{15}$$

with

$$C_i' = C_i\left(1 + \frac{a}{b}\right)^i. \tag{16}$$

B. Inverted Microstrip

Again defining

$$x = \frac{1}{u} = \frac{b}{w} \tag{17}$$

one gets

$$\frac{\ln\left(6x + \sqrt{1+4x^2}\right)}{F(x)} = \frac{Z}{60} \tag{18}$$

where

$$F(x) = 1 + \frac{x^3\left(\sqrt{\epsilon_r} - 1\right)}{C_0 x^3 + C_1 x^2 + C_2 x + C_3}. \tag{19}$$

Both (14) and (18) can be solved for x by using any of the well-known techniques for finding zeros of transcendental functions. For example, an application of the Newton-Raphson procedure (as in [3] and [4]) with initial guess

$$x = \frac{3g - \sqrt{g^2+8}}{16} \tag{20}$$

where

$$g = \exp(Z/60) \tag{21}$$

leads to the desired solution within a few iterations. Once x is known, W/b can be computed using (13) or (17), as the case may be.

A remark concerning the relevance of the synthesis equations (14) and (18) is in order. One usual CAD technique for synthesizing the planar transmission lines consists of putting the available analytical model in an iteration loop which adjusts the strip width until the desired impedance value is realized. Such a process, although without any synthesis error, lacks an initial guess and generally requires a large number of iterations. The present synthesis equations, on the other hand, converge to the desired impedance value within a few (typically five or fewer) iterations, and a slight loss in synthesis accuracy (less than 0.4 percent in the worst case, as will be discussed in the next section) is probably not an unreasonable price to pay for that.

IV. Modeling Accuracy

A. Analysis

The analysis equations were found to be accurate to within 0.6 percent of the exact theoretical data (both for Z and $\sqrt{\epsilon_{re}}$) over the range $1 \leqslant \epsilon_r \leqslant 20$, $0.5 \leqslant W/b \leqslant 10$, and $0.06 \leqslant a/b \leqslant 1.5$. The theoretical data used for comparison were generated for $t = 5$ μm, which is a very commonly used commercial value. Even if t is different from 5 μm and is in the practical range $0 \leqslant t/b \leqslant 0.02$, the results can be expected to be valid within 1 percent for $\sqrt{\epsilon_{re}}$ and within 2.5 percent for Z, since the effects of t are quite moderate in this t range [7].

B. Synthesis

The synthesis error arises from using (12) in place of (8), the upshot of which is that the W/b value obtained through solving the synthesis equation, when put back into the analytical model, yields a Z value slightly different from the one desired. The difference between the desired and realized Z values is termed the synthesis error.

For suspended line, the synthesis error increases with W/b, decreases with a/b, and is more or less insensitive to changes in ϵ_r [4]. The worst-case error of about 0.32 percent occurs at $W/b = 10$, $a/b = 0.5$. This, coupled with the expected error of the analytical model involved, makes the synthesis eq. (14) accurate to within about 1 percent of the exact Z value.

For inverted line, the synthesis error increases with W/b and is practically independent of a/b and ϵ_r [4]. The worst-case error of about 0.35 percent occurs at $W/b = 10$, so that the estimated accuracy of the synthesis eq. (18) is again about 1 percent.

V. Examples

In this section, some examples to illustrate the use of the above models are presented. The computations were made on a VAX 11/780 minicomputer.

A. Analysis

Let us first take the case of a suspended line on alumina substrate ($\epsilon_r = 9.6$) and with $a/b = 0.8$. The modeled values of $\sqrt{\epsilon_{re}}$ and Z are compared with the exact data in Table I. The agreement is better than 0.3 percent for both $\sqrt{\epsilon_{re}}$ and Z.

Next, consider an inverted line with $a/b = 1$ and deposited on GaAs substrate ($\epsilon_r = 12.9$). The results are shown in Table II and the agreement is again excellent (better than 0.5 percent).

B. Synthesis

The synthesis results for a suspended line with $\epsilon_r = 20$ (a hypothetical substrate) and $a/b = 1.2$ are shown in Table III. The agreement between desired and realized Z values is better than 1 percent, except when W/b goes below 0.5.

Table IV give the synthesis results for an inverted line with $\epsilon_r = 20$ and $a/b = 0.2$. The agreement is again better than 1 percent provided $W/b \geqslant 0.5$.

The z values in the third column of Tables III and IV are the exact theoretical data computed with the W/b value taken from the second column of the table. It also needs to be pointed out that all the results in Tables I–IV are rounded-off versions of the computer results, although the computations were made with an eight-digit accuracy.

TABLE I
Analytical Results for a Suspended Line

	$\sqrt{\epsilon_{re}}$		Z (Ohm)	
W/b	Eq. (1)	exact	Eq. (5)	exact
0.5	1.7097	1.7136	118.01	117.75
1.0	1.6370	1.6325	98.10	98.37
2.0	1.5404	1.5361	78.27	78.49
3.0	1.4804	1.4783	66.52	66.62
4.0	1.4405	1.4395	58.21	58.25
5.0	1.4128	1.4120	51.88	51.91
6.0	1.3929	1.3918	46.84	46.88
7.0	1.3781	1.3765	42.72	42.77
8.0	1.3667	1.3648	39.30	39.35
9.0	1.3572	1.3555	36.40	36.45
10.0	1.3487	1.3481	33.93	33.95

$\epsilon_r = 9.6$, $a/b = 0.8$.

TABLE II
Analytical Results for an Inverted Line

	$\sqrt{\epsilon_{re}}$		Z (Ohm)	
W/b	Eq. (9)	exact	Eq. (5)	exact
0.5	1.7551	1.7634	95.05	94.60
1.0	1.6344	1.6322	77.40	77.51
2.0	1.4780	1.4767	60.28	60.33
3.0	1.3815	1.3811	50.55	50.56
4.0	1.3164	1.3160	43.88	43.89
5.0	1.2698	1.2694	38.91	38.92
6.0	1.2349	1.2344	35.01	35.03
7.0	1.2080	1.2075	31.86	31.87
8.0	1.1866	1.1862	29.24	29.25
9.0	1.1694	1.1690	27.03	27.04
10.0	1.1553	1.1549	25.14	25.15

$\epsilon_r = 12.9$, $a/b = 1$.

TABLE III
Synthesis Results for a Suspended Line

Desired Z (Ohm)	Required W/b (Eq. (14))	Realized Z (Ohm)
30	11.64	29.81
40	7.01	39.96
50	4.41	49.87
60	2.78	59.88
70	1.73	69.94
80	1.07	79.88
90	0.67	89.40
100	0.43	98.08

$\epsilon_r = 20$, $a/b = 1.2$.

TABLE IV
SYNTHESIS RESULTS FOR AN INVERTED LINE

Desired Z (Ohm)	Required W/b (Eq. (14))	Realized Z (Ohm)
20	14.47	20.15
30	8.62	30.04
40	5.69	39.99
50	3.95	49.93
60	2.81	59.88
70	2.02	69.85
80	1.45	79.85
90	1.03	89.83
100	0.73	99.66
110	0.51	109.11
120	0.36	118.04

$\epsilon_r = 20, a/b = 0.2$.

VI. CONCLUSIONS

New CAD models for unshielded suspended and inverted microstrips are presented. These new models can be used up to $\epsilon_r = 20$ and also cover the entire dimension range that can conceivably be used in practice.

APPENDIX
EXPRESSIONS FOR d's

A. Suspended Line

Defining

$$f = \ln \epsilon_r \tag{A1}$$

we have

$$d_{00} = (176.2576 - 43.1240f + 13.4094f^2 - 1.7010f^3) \times 10^{-2} \tag{A2a}$$

$$d_{01} = (4665.2320 - 1790.4000f + 291.5858f^2 - 8.0888f^3) \times 10^{-4} \tag{A2b}$$

$$d_{02} = (-3025.5070 - 141.9368f - 3099.4700f^2 + 777.6151f^3) \times 10^{-6} \tag{A2c}$$

$$d_{03} = (2481.5690 + 1430.3860f + 10095.5500f^2 - 2599.1320f^3) \times 10^{-8} \tag{A2d}$$

$$d_{10} = (-1410.2050 + 149.9293f + 198.2892f^2 - 32.1679f^3) \times 10^{-4} \tag{A2e}$$

$$d_{11} = (2548.7910 + 1531.9310f - 1027.5200f^2 + 138.4192f^3) \times 10^{-4} \tag{A2f}$$

$$d_{12} = (999.3135 - 4036.7910f + 1762.4120f^2 - 298.0241d^3) \times 10^{-6} \tag{A2g}$$

$$d_{13} = (-1983.7890 + 8523.9290f - 5235.4600f^2 + 1145.7880f^3) \times 10^{-8} \tag{A2h}$$

$$d_{20} = (1954.0720 + 333.3873f - 700.7473f^2 + 121.3212f^3) \times 10^{-5} \tag{A2i}$$

$$d_{21} = (-3931.0900 - 1890.7190f + 1912.2660f^2 - 319.6794f^3) \times 10^{-5} \tag{A2j}$$

$$d_{22} = (-532.1326 + 7274.7210f - 4955.7380f^2 + 941.4134f^3) \times 10^{-7} \tag{A2k}$$

$$d_{23} = (138.2037 - 1412.4270f + 1184.2700f^2 - 270.0047f^3) \times 10^{-8} \tag{A2l}$$

$$d_{30} = (-983.4028 - 255.1229f + 455.8729f^2 - 83.9468f^3) \times 10^{-6} \tag{A2m}$$

$$d_{31} = (1956.3170 + 779.9975f - 995.9494f^2 + 183.1957f^3) \times 10^{-6} \tag{A2n}$$

$$d_{32} = (62.8550 - 3462.5000f + 2909.9230f^2 - 614.7068f^3) \times 10^{-8} \tag{A2o}$$

$$d_{33} = (-35.2531 + 601.0291f - 643.0814f^2 + 161.2689f^2) \times 10^{-9} \tag{A2p}$$

B. Inverted Line

Again defining f as in (A1), we get

$$d_{00} = (2359.4010 - 97.1644f - 5.7706f^2 + 11.4112f^3) \times 10^{-3} \tag{A3a}$$

$$d_{01} = (4855.9472 - 3408.5207f + 15296.7300f^2 - 2418.1785f^3) \times 10^{-5} \tag{A3b}$$

$$d_{02} = (1763.3400 + 961.0481f - 2089.2800f^2 + 375.8805f^3) \times 10^{-5} \tag{A3c}$$

$$d_{03} = (-556.0909 - 268.6165f + 623.7094f^2 - 119.1402f^3) \times 10^{-6} \tag{A3d}$$

$$d_{10} = (219.0660 - 253.0864f + 208.7469f^2 - 27.3285f^3) \times 10^{-3} \tag{A3e}$$

$$d_{11} = (915.5589 + 338.4033f - 253.2933f^2 + 40.4745f^3) \times 10^{-3} \tag{A3f}$$

$$d_{12} = -1957.3790 - 1170.9360f + 1480.8570f^2 - 347.6403f^3) \times 10^{-5} \tag{A3g}$$

$$d_{13} = (486.7425 + 7425 + 279.8323f - 431.3625f^2 + 108.8240f^3) \times 10^{-6} \tag{A3h}$$

$$d_{20} = (5602.7670 + 4403.3560f - 4517.0340f^2 + 743.2717f^3) \times 10^{-5} \tag{A3i}$$

$$d_{21} = (-2823.4810 - 1562.7820f + 3646.1500f^2 - 823.4223f^3) \times 10^{-5} \tag{A3j}$$

$$d_{22} = (253.8930 + 158.5529f - 3235.4850f^2 - 919.36661f^3) \times 10^{-6} \tag{A3k}$$

$$d_{23} = (-147.0235 + 62.4342f + 887.5211f^2 - 270.7555f^3) \times 10^{-7} \tag{A3l}$$

$$d_{30} = (-3170.2100 - 1931.8520f + 2715.3270f^2 - 519.3420f^3) \times 10^{-6} \tag{A3m}$$

$$d_{31} = (596.3251 + 188.1409f - 1741.4770f^2 + 465.6756f^3) \times 10^{-6} \quad \text{(A3n)}$$

$$d_{32} = (124.9655 + 577.5381f + 1366.4530f^2 - 481.1300f^3) \times 10^{-7} \quad \text{(A3o)}$$

$$d_{33} = (-530.2099 - 2666.3520f - 3220.0960f^2 + 1324.4990f^3) \times 10^{-9}. \quad \text{(A3p)}$$

REFERENCES

[1] P. Pramanick and P. Bhartia, "Analysis and synthesis of suspended and inverted microstrip lines," *Arch. Elek. Übertragung*, vol. 39, pp. 23–26, 1985.

[2] P. Pramanick and P. Bhartia, "Computer-aided design models for millimeter-wave finlines and suspended substrate microstrip lines," *IEEE Trans. Microwave Theory Tech.*, vol. MTT-33, pp. 1429–1435, Dec. 1985.

[3] R. S. Tomar and P. Bhartia, "A new accurate method of synthesising suspended and inverted microstrip lines," in *Conf. Proc., IEEE ELECTRONICOM'85* (Toronto, Canada), Oct. 1985, pp. 574–577.

[4] R. S. Tomar and P. Bhartia, "Suspended and inverted microstrip design," *Microwave J.*, vol. 29, no. 3, pp. 173–178, Mar. 1986.

[5] R. S. Tomar and P. Bhartia, "Effects of manufacturing tolerances on the electrical performance of suspended and inverted microstrip lines," *Int. J. Infrared & MM Waves*, vol. 6, no. 9, pp. 807–829, Sept. 1985.

[6] E. Yamashita, "Variational method for the analysis of microstrip-like transmission lines," *IEEE Trans. Microwave Theory Tech.*, vol. MTT-25, pp. 648–656, Mar. 1977.

[7] S. Koul and B. Bhat, "Characteristic impedance of microstrip-like transmission lines for millimeter-wave applications," *Arch. Elek.* Übertragung, vol. 35, pp. 253–258, 1981.

[8] E. Hammerstad and O. Jensen, "Accurate models for microstrip computer-aided design," in *IEEE MTT-S Symp. Dig.*, 1980, pp. 407–409.

[9] P. Bhartia and I. J. Bahl, *Millimeter-Wave Engineering and Applications*. New York: Wiley, 1984, p. 276 (eq. 6.24).

A Study of Measurements of Connector Repeatability Using Highly Reflecting Loads

JOHN R. JUROSHEK, MEMBER, IEEE

Abstract—**This paper investigates the repeatability of measurements of the reflection coefficient Γ of highly reflecting devices with changes in the RF connector joint. The changes in the connector joint are due to disconnecting and reconnecting the connector pair. It is shown that many of the measurement discrepancies observed in practice can be explained with a simple connector model. The paper shows that the sensitivity of measuring RF connector changes can be increased by using highly reflecting loads. The changes in Γ due to changes in resistance or reactance can be four times greater for highly reflecting devices ($|\Gamma| \approx 1$) than for nonreflecting devices ($|\Gamma| \approx 0$). Experiments on two devices with 14-mm connectors are described in order to compare them with theory. The basic principles described in this paper should be beneficial to connector designers who need to observe small changes in connector parameters and to the work of calibration standards designers, where small connector imperfections are a major part of their measurement uncertainty.**

I. INTRODUCTION

It has been recognized for some time that coaxial connectors limit the accuracy of many of the measurements at microwave frequencies. It is difficult to make measurements with today's modern network analyzer and not be acutely aware of connectors and their lack of repeatability. Recent studies at the National Bureau of Standards have been successful in developing an improved connector model and in developing a technique for measuring parameters for that model [1]. This paper examines the implications of that model on the measurements of the reflection coefficient Γ of highly reflecting devices ($|\Gamma| \approx 1$). In particular, this paper investigates the repeatability of measurements of Γ with changes in the RF connector joint parameters. The changes in Γ due to changes in resistance, or reactance at the connector's center conductor joint, are described. It is shown that the changes in Γ can be up to four times greater for highly reflecting devices than for the nonreflecting case ($|\Gamma| \approx 0$). The changes in Γ are frequency dependent and are greatest at or near the maximum current ($\arg(\Gamma) = 180°$) or the current null ($\arg(\Gamma) = 0°$) frequencies. The basic principles described in this paper should be beneficial to connector designers who need to observe small changes in connectors and in the design of calibration standards, where connector imperfections are a major part of the measurement uncertainty.

II. THEORY

Consider the circuit shown in Fig. 1, composed of a connector with joint scattering parameters S_{ij}, a coaxial transmission line of length l, and a termination Γ_T. This connector joint model and methods for determining S_{ij} are described in a paper by Daywitt [1]. The reflection coefficient Γ looking into this combination is given by

$$\Gamma = S_{11} + \frac{S_{12}^2 \Gamma_l}{1 - S_{22}\Gamma_l} \quad (1)$$

where Γ_l is the reflection coefficient looking into the transmission line. The scattering parameters for the connector joint are given in [1] as

$$S_{11} = S_{22} = \frac{r}{2} + \frac{x}{2} - y \quad (2)$$

$$S_{12} = S_{21} = 1 - \frac{r}{2} - \frac{x}{2} - y \quad (3)$$

where r is the normalized joint resistance:

$$r = R/Z_0 \quad (4)$$

x is the normalized joint reactance:

$$x = j\frac{2\pi f L}{Z_0} \quad (5)$$

and y is the normalized joint admittance:

$$y = j2\pi f C Z_0. \quad (6)$$

The joint's length is assumed to be small relative to a wavelength. Substituting (2) and (3) into (1) and eliminating second-order terms in r, x, and y results in

$$\Gamma = \Gamma_l + (1 - \Gamma_l)^2 \frac{r}{2} + (1 - \Gamma_l)^2 \frac{x}{2} - (1 + \Gamma_l)^2 y. \quad (7)$$

Therefore, the change in Γ due to changes in r, x, or y is given by

$$\frac{\partial \Gamma}{\partial r} = \frac{(1 - \Gamma_l)^2}{2} \quad (8)$$

$$\frac{\partial \Gamma}{\partial x} = \frac{(1 - \Gamma_l)^2}{2} \quad (9)$$

Manuscript received July 24, 1986; revised November 29, 1986.

The author is with the Electromagnetic Fields Division, National Bureau of Standards, Boulder, CO 80303.

IEEE Log Number 8613288.